PROCEEDINGS, 42nd Workshop on Geothermal Reservoir Engineering
Stanford University, Stanford, California, February 13-15, 2017
SGP-TR-212

Re-evaluating Thermal Conductivity from the Top Down: Thermal Transport Properties of Crustal Rocks as a Function of Temperature, Mineralogy and Texture

Jesse D. Merriman[1], Alan G. Whittington[1], and Anne M. Hofmeister[2]

[1]Department of Geological Sciences, The University of Missouri, 101 Geology Building, Columbia, MO 65203

[2]Department of Earth and Planetary Sciences, Washington University, One Brookings Drive, St. Louis, MO 63130

jdm42c@mail.missouri.edu

Keywords: Thermal Diffusivity, Thermal Conductivity, Heat Flow, Thermal Modeling, Geothermal Gradient

ABSTRACT

Accurate modeling and forecasting of potential geothermal resources requires accurate measurements or predictions of the physical properties of the crust. The conductive thermal transport properties of rocks, thermal conductivity (*k*) and thermal diffusivity (*D*), have been studied extensively for over a hundred years, but it has been shown that results obtained by commonly used techniques contain systematic errors associated with imperfect contacts and ballistic radiative transfer (heat transport by radiation that does not interact with or warm the sample, and is directly generated by the heating element). Using Laser Flash Analysis (LFA), which limits these systematic errors, we have measured the temperature-dependent thermal diffusivity of major rock types across relevant lithospheric temperatures. These experiments have shown that *D* is much higher at low temperatures, and much lower at high temperatures than previous methods suggested. The temperature-dependence of *D* is therefore very strong (typically a factor of 2 to 5 over the range 20 to 500˚C), and *D* of common crustal minerals and rocks can vary by a factor of 4 or more at ambient temperatures.

Thermal diffusivity of common crustal rock types can vary by a factor of 4 or more at ambient temperatures, and even by a factor of 2 for a given rock type. Variability between rocks of the same category may result from differences in modal abundances of rock-forming minerals, or contrasts in textures such as pore fraction. The combination of mineralogical, textural and temperature controls make predicting rock *D* by broadly-defined rock types (e.g. granite, basalt, marble) a potentially large source of error. For *k*, variability is even more complex because it is the product of *D*, heat capacity, and density, all of which are controlled by several properties. Accurate prediction of thermal transport properties requires petrographic (mineralogical and textural) investigation, and the effects of each property. The strong temperature-dependence of thermal transport properties, especially between ambient and ~500˚C, introduces the potential for feedbacks between heating and thermal insulation in the crust, an effect which needs to be incorporated in models when prospecting geothermal resources.

1. INTRODUCTION

As new technologies developed for geothermal energy production broaden its application from traditional naturally convective sources, to hot-dry-rock resources, the role of thermal conduction in the prospecting and development of geothermal resources will increase significantly. The development of deep-seated convective sources and the understanding of the broader thermal systems involved require a strong understanding of the ability of the materials involved to conduct heat. Given that drilling is expensive, and likely to remain so for the foreseeable future, prospecting for geothermal resources in the 21st century will require robust models of the thermal structure of a potential resource.

Conductive heat flow depends on thermal conductivity (k), thermal diffusivity (D), heat capacity (C_P) and density (ρ) which are related through the equation $k = D\rho C_P$.These properties vary with rock type, temperature, and porosity, as is long known (see Clauser and Huenges, 1995 or Hantschel and Kauerauf, 2009 for summaries.) Additionally, these properties are pressure-dependent, although in the lithosphere, decreases in ρ due to increasing temperature are relatively small, and largely offset by increasing pressure with depth (Hofmeister, 2007).

Fourier's law describes how the flux of heat relates to temperature and material properties. In Cartesian coordinates, and at steady-state):

$$\dot{q} = -k\frac{dT}{dz} \quad (1)$$

where $\dot{q}$ is heat flux ($\mathrm{Wm^{-2}}$), dT/dz is the temperature gradient ($\mathrm{Km^{-1}}$). If heat flux is constant, eq. 1 shows that a higher gradient is sustained by a low-k material, and conversely, a high-k material cannot maintain a high temperature gradient. Furthermore, constant k means that the thermal gradient is linear (in the absence of a source of internal heat). In natural materials, however, k is not constant. This variable k greatly complicates attempts to ascertain the temperature gradient associated with a defined heat flux:

$$\frac{dT}{dz} = -\frac{\dot{q}}{k(T)} \quad (2)$$

where *k(T)* denotes *k* as a function of temperature. For example, if $q = 50$ mW/m^2, and *k* of a rock is 3.0 Wm^{-1}K^{-1} at 25°C, then dT/dz = 17 °C/km. However, if the same rock has a *k* of 1.5 Wm^{-1}K^{-1} at 200°C, then dT/dz would double to 33 °C/km. Real-world geothermal gradients are more complex, in part because radioactive decay in the crust provides additional heat. In the absence of this heating, the geothermal gradient would be lower at the surface and likely increase with depth.

Given the above, the time-dependence of heat flow can be very complex. To calculate the thermal evolution of conducting layers, models typically rely on thermal diffusivity because this isolates the flow of heat from the amount of heat moved. Like *k*, *D* is typically moderately- to highly- temperature-dependent, and varies strongly by material (e.g. Birch and Clark, 1940; Robertson, 1988; Clauser and Huenges, 1995; Whittington *et al.,* 2009; Hofmeister and Branlund, 2015). Models which incorporate temperature-dependent *D* or *k* often produce results that are very different from those that use invariant transport properties. Nabelek *et al.* (2012) compared cooling rates of a 50 m thick basaltic sill at liquidus temperatures (1230°C) emplaced in country rock at 150°C. Using temperature-dependent *D* effectively doubled the cooling time of the sill compared to using invariant *D*. This occurred because heat from the sill increased the temperature of the surrounding rock. *D* of most rocks decreases with increasing temperature, which in this model caused a feedback relationship between heat from the sill and the ability of the country rock to dissipate that heat. On a larger scale, Whittington *et al.* (2009) modeled continental collision using *T*-dependent *D*, and found that feedback between strain-heating and more insulating rocks reduced the need for high radioactive element concentrations within the crust to generate large-scale crustal melting as previous models had suggested.

Figure 1 shows the effects of variable temperature on the overall ability of an ad hoc crust to conduct heat. The upper 10 km of a crust composed of three layers: 3 km of limestone (sample MO-05, Merriman *et al.*, under review), 3 km of greenschist facies metavolcanic rock (chloritized komatiite TF07, Merriman *et al.*, 2013), and 6 km of tonalite (KB12ab, Merriman *et al.,* 2013). This profile illustrates the effects of 3 types of hypothetical geothermal gradients: a "cold" linear geotherm similar to thick, cold cratonic lithosphere (20°C/km), a "hot" linear geotherm (50°C/km) and a "hot" curved geothermal gradient. The last two could result from rifting, a lower layer with very high internal heat production, or emplacement of a pluton, etc. The ability of the crust to conduct heat changes dramatically between the 20°C/km geotherm and the hot geotherms. For example, in the upper tonalite layer, *D* is ~1.8 mm^{2}s^{-1} when the geothermal gradient is low, but increasing the gradient lowers the *D* at the same spot to ~1.2 mm^{2}s^{-1}. In this example the geotherms are independent of *D* (and *k*), but in reality, the geotherm would change in response to these changes in *D* (and vice versa). The shape of the curved geotherm is more in line with models of the geothermal gradient in continental crust, but models which use multiple layers of rock with different thermal transport properties typically find the slope of the geotherm changes where two layers meet.

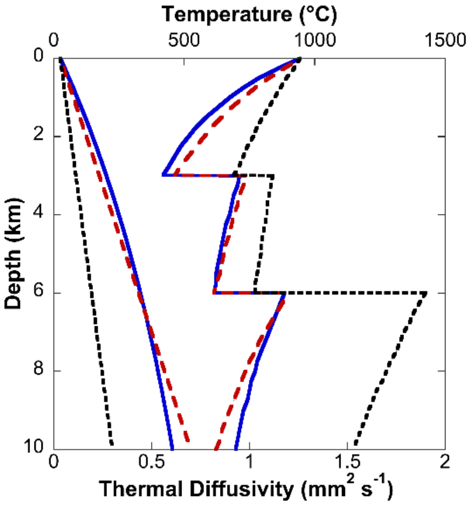

Figure 1) Thermal conduction profiles (right side) resulting from 3 hypothetical geothermal gradients (left side). Short-dashed lines are for a 20°C/km geotherm, long-dashed lines for a 50°C/km geotherm, and solid lines are a variable geotherm with higher *dT/dz* in the shallower crust. Upper crust is limestone, middle crust low-grade metavolcanic rocks, and lower crust tonalite (plagioclase-dominated granitoid). References in text.

Given the importance of *k* to thermal conduction within the Earth, it is essential that modern modeling incorporates accurate, and carefully selected values for *D* and *k.* This paper reviews the current state of thermal transport property measurement and analysis, evaluates the properties of rocks that govern conductive thermal transport, and explores how recent evolution of *D* measurements may lead to better models for calculating *D* and *k* when direct measurement to appropriate temperatures is impractical or unavailable.

2. THE MEASUREMENT AND CALCULATION OF THERMAL DIFFUSIVITY AND RELATED PROPERTIES

Heat capacity of a rock, and its change with temperature, can be accurately calculated using well-characterized modal mineralogy of a rock under analysis (e.g. Robie & Hemingway, 1995). Likewise, density requires simple, cost-effective methods to directly measure, but can also be accurately calculated using mineral densities combined with porosity, and in some cases, end-member proportions for minerals with solid solutions (e.g. forsterite (density= ~3.3 g/m^3) vs fayalite (density = ~4.4 g/m^3). Thermal conductivity and thermal diffusivity, however, are more problematic to calculate, as multiple textural and mineralogical properties influence bulk-rock *D* and *k.*

Additionally, error associated with calculating these at low temperature is often propagated when extrapolating to elevated temperatures (e.g. Merriman *et al.,* Under Review). This section reviews experimental errors common to popular techniques that directly measure k, and introduces Laser Flash Analysis (LFA) as a method which can control for these errors.

2.1 Experimental error in k measurement

Standard methods for measurement of thermal conductivity are often influenced by experimental error in the form of contact loss at low-temperature, and ballistic radiative transfer (i.e. direct radiative transfer that does not interact with or warm the sample, especially common in lab experiments on a small scale with transparent materials) at elevated temperatures (Hofmeister, 2008). When physical contacts are present in a measurement, microscopic imperfections in the sample surface create void spaces which do not conduct heat (Branlund and Hofmeister, 2008; Whittington *et al.,* 2009). This typically results in lower-k reported than the sample would produce under confining pressure, typically ~10% per physical contact, but often not reproducible (Ross *et al*., 1984). Additionally, many minerals are transparent in the near-IR, and light generated by the heating element (ballistic radiative transfer) travels through the sample without interaction with it, leading to higher k than occurs in nature. Because radiative flux is generated as T^4, the contribution of this ballistic radiative transfer is most significant at elevated temperatures (Hofmeister, 2010a).

2.2 Methods that control for common experimental error

Laser flash analysis (LFA) was first developed in the 1960's (Parker *et al.,* 1961), and removed errors associated with physical contacts but did not control for ballistic radiative transfer at elevated temperatures until the algorithm of Mehling *et al.* (1998). The LFA directly measures *D* of samples in a controlled atmosphere (usually Ar) which can be heated to temperatures as high as 1500°C. A laser pulse on the lower surface of a sample disk (typically ~1cm in diameter, and 0.5-10mm in thickness) heats the sample, and the time required for the heat to diffuse through the sample is measured. Ballistic radiative transfer in LFA experiments is apparent by a (near) instantaneous increase in temperature measured by an IR detector on the opposite side of the sample, and then removed from the data using the appropriate algorithm. Other non-contact methods such as the Popov method (Popov *et al.*, 1999) exist and were developed fairly recently, but are limited to room-temperature, or are less widely used.

3. THERMAL DIFFUSIVITY OF MINERALS

Over the past decade, the *D* of most of the major rock forming minerals have been measured to high-temperatures (typically at or near the melting point of the mineral at atmospheric pressure). This data set includes garnets (Hofmeister, 2006), olivines (Pertermann and Hofmeister, 2012), spinels and magnetite (Hofmeister, 2007), quartz (Branlund and Hofmeister, 2007), clinopyroxenes (Hofmeister and Pertermann, 2008), potassium feldspars (Pertermann *et al.,* 2008; Hofmeister *et al.,* 2009), oxide perovskites (Hofmeister, 2010b), alkali and silver halides (Yu and Hofmeister, 2011), orthopyroxenes (Hofmeister, 2012), plagioclase feldspars (Branlund and Hofmeister, 2012), fluorite, diamond and graphite (Hofmeister *et al.,* 2014), periclase and corundum-structure oxides (Hofmeister, 2014), micas (Hofmeister and Carpenter, 2015), feldspathoids and zeolites (Hofmeister and Ke, 2015), and carbonates (Merriman *et al.,* under review). Data have been collected for amphiboles and chlorites, but are not yet published.

Reviewing the substantial database generated by measurement of minerals with the LFA, Hofmeister *et al.* (2014) proposed that data for the temperature-dependence of mineral thermal diffusivity can be fit to:

$$D(T) = FT^{-G} + HT \tag{3}$$

where F, G and H are constants that depend on mineral composition and structure. The HT term describes solely diffusive radiative transfer in the infrared (specifically polaritons, see Hofmeister *et al.*, 2014). This process offsets the decrease in *D* at high temperature, which typically results in near temperature-independent *D* as the temperature of the mineral approaches its melting point. Diatomic substances such as NaCl (Halite), and the mineral corundum (Al_2O_3) typically do not include the H term, and thus have a greater decrease in D at elevated temperatures (Yu and Hofmeister, 2011). Conversely, the *D* of Fe_2O_3 appears to reach a minimum around ~1000K, and then increase. Instead of an HT term, fits for Hematite include a much stronger CT^3 term (Hofmeister, 2014; Hofmeister *et al.,* 2014). Hofmeister *et al.* (2014) includes fitting parameters for most of the above minerals (fitting parameters for the micas and carbonates are presented in later papers as mentioned above).

Figure 2 shows the change in *D* of several common rock-forming minerals. Typically, the change in *D* with temperature (*dD*/*dT*) is high in the temperature range ~300-600K, after which *dD*/*dT* decreases until the sample *D* approaches an asymptote close to the mineral's melting point. The consequence of this is that at near-surface temperatures, the ability of a mineral to conduct heat may be as much as five times higher at room-temperature than near its melting temperature. For example, the Mg-endmember of olivine, forsterite (heat flow along [001]), has a room-temperature *D* of ~5.1 $mm^2\ s^{-1}$. At 600 K, *D* has dropped by ~60% to ~2.0 $mm^2\ s^{-1}$, and by 1200 K, *D* reaches an apparent asymptote near ~1.0 $mm^2\ s^{-1}$ (Pertermann and Hofmeister, 2006).

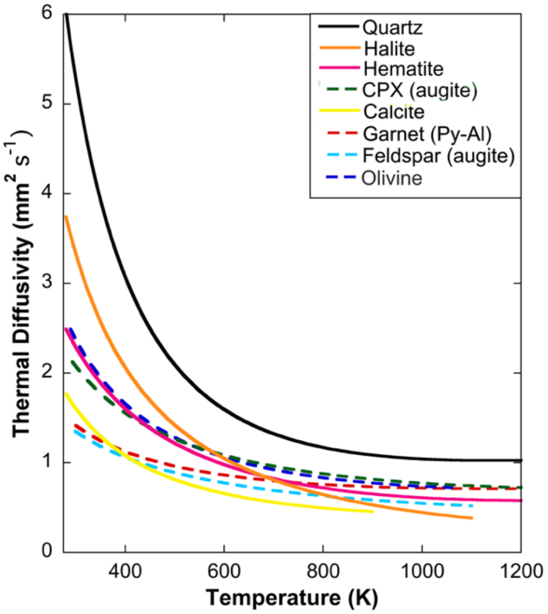

Figure 2) Thermal diffusivity of some common rock-forming minerals. Data are from references in text. Dashed lines are minerals with solid solutions, see discussion in text. Samples with different crystal orientations are directionally averaged. Trends are broadly similar, with the diatomic substance NaCl showing a lack of an HT term at high temperatures. References in text (Section 3).

Thermal diffusivity also depends on orientation of the crystal and, in minerals with solid-solutions, the proportions of endmembers in the mineral. For example, the clinopyroxene diopside ($CaMgSi_2O_6$) has a directionally averaged *D* of 3.4 mm^{2}s^{-1} at 280 K, falling to 1.0 mm^2 s^{-1} at 1000 K (figure 2). However, heat flow along [100] (2.7 mm^{2}s^{-1} at 280 K, 0.6 mm^{2}s^{-1} at 1000 K) is comparatively lower than along [001] (4.1 mm^{2}s^{-1} at 280 K, 1.3 mm^{2}s^{-1} at 1000 K). Substitution of moderate amounts of Fe and Al for Mg (Diopside vs. Augite) increases cation disorder in the crystal, effectively lowering the *D* of the mineral: Directionally averaged Augite has a *D* of 2.2 mm^2 s^{-1} at 280 K and 0.8 mm^2 s^{-1} at 1000 K. Figure 3 shows *D* for several clinopyroxenes, illustrating the effects of cation disorder (substitution) and crystal orientation. Most mineral groups with anisotropic dimensions show moderate-to-strong dependence on orientation of the crystal. However, this effect was not visible in carbonate minerals where *D* values varied by <3% between orientations (Merriman *et al.,* under review). Conversely, Hofmeister and Carpenter (2015) found mica *D* varied by roughly an order of magnitude between orientations (e.g. heat flow within layers of phlogopite, 2.29 mm^2 s^{-1} (295.2 K), across layers 0.172 mm^2 s^{-1} (294.6 K)). This difference relates to weak bonding and large separations between layers in the structure: however, the low values are obviously affected by poor thermal contact between cleavage planes, the latter effect which would disappear under confining pressure.

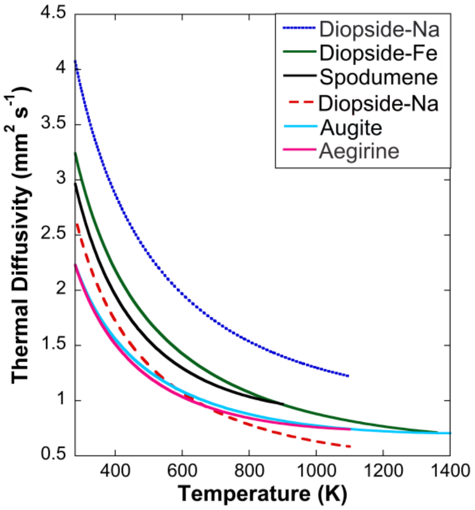

Figure 3) Thermal diffusivity of several clinopyroxenes. Samples Diopside-Fe, Aegirine, and spodumene are directionally averaged. Dashed lines indicate heat flow along [100], dotted lines heat flow along [001]. Variations in *D* between orientations for other end-members of cpx are similarly high (Hofmeister and Pertermann, 2008).

4. THERMAL CONDUCTIVITY OF MINERALS

Thermal diffusivity of minerals can be used to calculate thermal conductivity if the heat capacity and density of the mineral are known. For minerals without solid-solutions such as calcite or quartz, published values can be used directly. For minerals such as the feldspars, which form solid solutions, C_P or density can be approximated by the weighted averaged of each proportion of end-member in the mineral.

The thermal diffusivity of minerals with solid-solutions is somewhat more complex, however. Dolomite is composed of alternating layers of $MgCO_3$ (magnesite, $D = 4.4$ mm^2 s^{-1} at 296 K) and $CaCO_3$ (calcite, D = 1.6 mm^2 s^{-1} at 296 K), leading to a room-temperature D of 2.7 mm^2 s^{-1} (Merriman *et al.,* under review). However, for minerals with extensive solid solutions (e.g. plagioclase feldspars or olivines), several factors complicate end-member D. Plagioclase, for example, has coupled substitution of Na and Ca, and Si and Al between albite ($NaAlSi_3O_8$) and anorthite ($CaAl_2Si_2O_8$). This coupled substitution causes structural disorder within the crystal, resulting in an initial high decrease in D when moving from pure albite to anorthite as Ca substitutes for Na. Rough approximation of endmember proportions within a mineral will produce roughly-correct D, but error is high (figure 4) and should be applied carefully based on the mineral solid solution. In general, minerals with complex solid solutions, however, tend to produce low D and a lower temperature-dependence to D, but also smaller variability in D between end-members (e.g. feldspars, garnets), which limits error associated with averaging endmembers when data is not available for an appropriate composition.

Calculated temperature-dependent k for minerals typically produces a non-linear decrease in k with increasing temperature. However, the interplay of temperature-dependent D and temperature-dependent C_P can result in more complex behavior than is seen with D. Mineral C_P generally increases with increasing temperature, rapidly at low temperature (typically ~300-600 K), but has a low T-dependence at higher temperatures (figure 4). Because C_P varies much less between minerals than D, minerals with very low-D and a low dD/dT can have resulting k that is relatively insensitive to temperature (Branlund and Hofmeister, 2012), occasionally even showing a small increase at low temperatures (see Ab51An47Or2, figure 4).

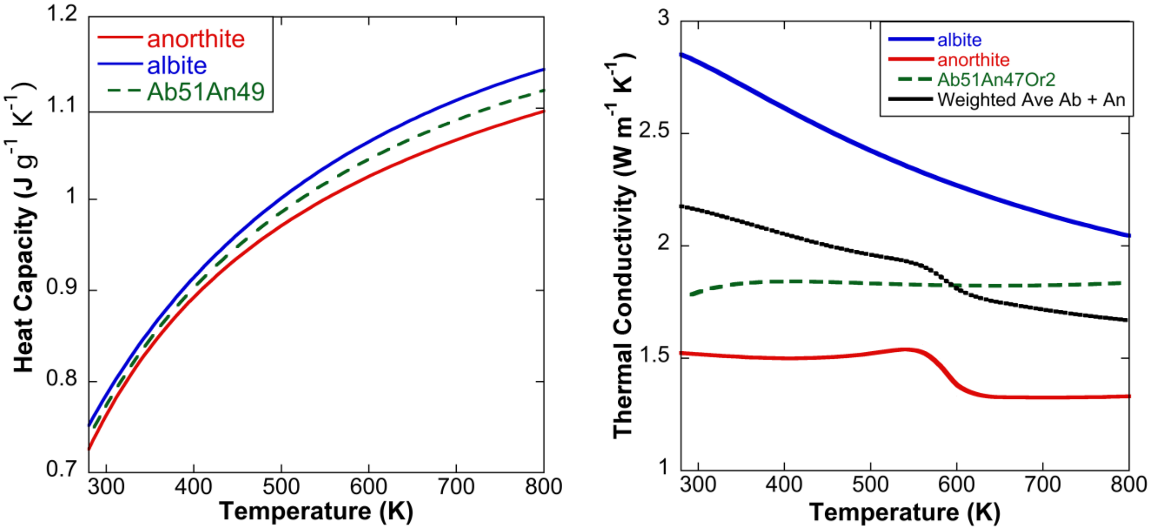

Figure 4) Isobaric heat capacity (a), and calculated thermal conductivity (b) of endmember albite, near-endmember anorthite, and Ab51An49, with *k* of Ab51An47Or2 (where Or denotes potassium feldspar) calculated from direct *D* measurement. Using the weighted average of Albite and Anorthite for Ab51An49 introduces error up to ~24% at low temperature because of different *dD/dT* patterns for endmember albite and anorthite. Potassium feldspar has similar *dD/dT* patterns to albite, with room-*T D* of ~~1.1 mm^{2}s^{-1}. References for *D* data in section 3. C_P data from Robie and Hemingway (1995).

5. THERMAL DIFFUSIVITY AND THERMAL CONDUCTIVITY OF ROCKS

Rocks measured with the LFA method typically have values of D of the same order of magnitude and similar temperature-dependence of mineral D, but additional factors make rock D more complicated. Figure 5 shows the thermal diffusivity of several rock types measured using the LFA method. Rocks composed of chiefly of high-D minerals produce relatively high-D at low temperatures (e.g. quartzite, Branlund and Hofmeister, 2008; dolomitic marble, Merriman *et al.,* under review), whereas those composed chiefly of low-D minerals show lower D (e.g. plagioclase-dominated granite, Miao *et al.,* 2014; metamorphic average of Nabelelk et al., 2010). However, at higher temperatures, contrasts in bulk-rock D narrow to the range 0.6-1.0 mm^2 s^{-1} above 700 K, decreasing only modestly at higher temperatures.

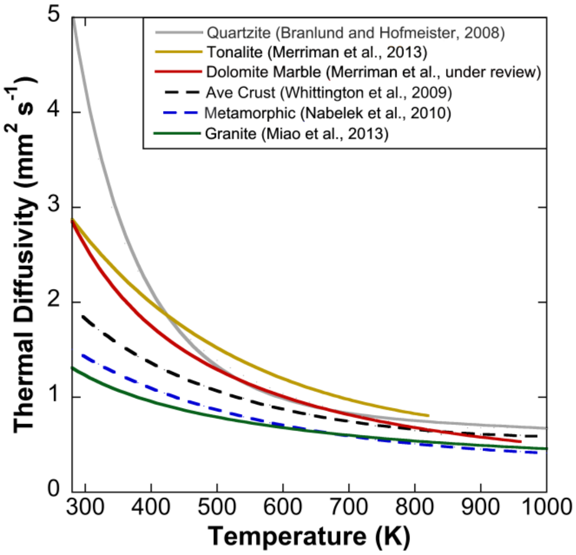

Figure 5) Thermal diffusivity of several rocks measured with the LFA method. Values from Whittington *et al.* (2009) and Nabelek *et al.* (2010) are averages of multiple samples. Low-*D* in the granite of Miao *et al.* may be a result of high plagioclase content, an effect which is not present in all granites.

Although bulk-rock *D* behaves similarly to mineral *D*, rock *D* is almost universally lower than the highest *D* mineral it contains, an effect which typically extends to monomineralic rocks (e.g. quartzites: Branlund and Hofmeister, 2008; limestones and cc-marbles: Merriman *et al.,* under review). This is because multiple properties combine to produce the effective *D* of a rock, including mineralogy and mineral proportions, grain size and grain-boundary resistance, and porosity and pore-filling material. A review of each effect follows.

5.1 Textural controls on bulk-rock thermal diffusivity and thermal conductivity

Much effort has been placed on exploring the effects of porosity on *k* in porous materials (e.g. Carson *et al.,* 2005; Schutz *et al.,* 2012), but extension of these efforts to bulk-rock *D* is complicated by competing effects due to rock density and C_P (Branlund and Hofmeister, 2008), and efforts for thermal conductivity are clouded by experimental uncertainties as described above. Some aspects of pore theory are applicable to *D* measurements with the LFA, however (e.g. Smith *et al.,* 2003). To explore these effects in rocks, we examined pore and textural effects for the carbonate suite of Merriman *et. al (*under review), and the quartzites of Branlund and Hofmeister (2008). Both these suites are ideally suited for examining textural influences on rock *D* and *k* because many of the samples are monomineralic, or dominated by a single mineral (>90% by volume).

5.1.1 Porosity and Pore-Filling Fluid

The fraction of pore space (ϕ) within a rock will lower the rock's effective *D* and *k* because (with few exceptions), mineral *D* is higher than the *D* of the material filling the pore space (e.g. Abramson *et al.,* 2001; Wang *et al.,* 2008). Typical pore-filling materials include air, water, brine, oil, and gas (Carson *et al.,* 2005; Branlund and Hofmeister, 2008). In addition to lower *D*, the heat transport properties of pore-filling fluids do not necessarily show the same response to temperature as crystalline minerals. For example, water *D* is ~0.14 mm^{2}s^{-1} at room-temperature, but *increases* with increasing temperature (0.17 mm^{2}s^{-1} at 110°C, Lawson, 1959), and pressure (0.19 mm^{2}s^{-1} at 1.1 GPa and 25°C, Abramson *et al.,* 2001). By comparison, pressure effects within minerals are typically small relative to the temperature response (Hofmeister, 2007).

The thermal diffusivity contribution of pore space and the materials that fill it can be determined if the porosity is well-characterized, and the bulk-rock D and matrix (solid) D are measured or calculated. D of pore spaces (D_{pore}) is given by the equation:

$$D_{rock} = \frac{1}{\frac{1-\phi}{D_{mx}} + \frac{\phi}{D_{pore}}} \tag{4}$$

where D_{rock} is the thermal diffusivity of the bulk rock, D_{mx} is the *D* of the matrix (mineral aggregate), and ϕ is the pore fraction (Smith *et al.,* 2003; Branlund and Hofmeister, 2008). Using the above equation, we calculated D of pore-spaces for the monomineralic carbonates of Merriman *et al.* (Under Review), and found D_{pore} between ~0.2 and 0.5 mm^{2}s^{-1}. These values are broadly consistent with pore-space filled with water, or brine, suggesting that pore space is largely isolated and filled. Branlund and Hofmeister (2008) performed the same analysis for a suite of quartzites and found much higher D_{pore} (typically 0.6-1.4 mm^{2}s^{-1}) and attributed higher D_{pore} to a dissolved phase in pore water.

A number of models for effective thermal *conductivity* of porous media as summarized by Carson *et al.* (2005) have been formulated. These models generate bulk-material (rock) *k* based on distribution of pore space within it. Boundaries of potential effects of porosity scale based on whether the pore space is effectively in series, in parallel, matrix-dominated, dispersed, or randomly distributed (Figure 6). Although these models generate rough bounds for the range of effective k for a rock, they do not predict the k_{eff} of the rock given a pore fraction. This is in part due to the diversity of possible k of pore-filling fluids, but may also be a consequence of the complex interplay of properties that govern heat flow in the rock. Additionally, the increased error associated with contact losses, ballistic radiative transfer at low temperatures for more transparent minerals within the rock, and variability in measurement methods given the diversity of instruments available for direct k measurement.

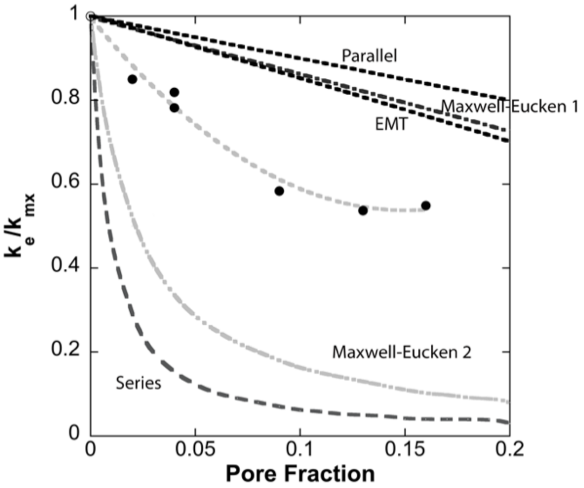

Figure 6) Graph of effective k (k_e) over matrix k (k_{mx}) versus pore fraction for a series of calcite-dominated limestones and marbles as described by Merriman *et al.* (under review).

5.1.2 Grain-Boundary Resistance

Grain boundaries create effective disorder within the structure of a rock, generating resistance to phonon propagation. For heat to have a net movement across a grain boundary, the pathway in the new grain must provide an easier path for heat to flow which is less than the dampening effect of the grain boundary resistance (Smith et al., 2003). Grain-boundary resistance (R) is on the order of 10^{-8} m^2 K W^{-1}, and generates a lower k_{eff} per the equation:

$$k_{eff} = \left(\frac{1}{k_{mx}} + \frac{n_l}{l} R\right)^{-1} \tag{5}$$

where n_l is the number of grain boundaries over an l (length in meters). In practice, grain boundary resistance is closely tied to grain-size.

5.1.3 Grain Size

Larger grains generally provide the potential for longer mean-free paths for heat to diffuse, but studies of D that include grain size generally do not find a strong dependence on grain size (e.g. Gibert *et al.,* 2003; Branlund and Hofmeister, 2008; Merriman *et al.*, under review). However, very fine-grained material dramatically increases the grain-boundary effect (Smith *et al.*, 2003), leading Branlund and Hofmeister (2008) to conclude that grain size affects bulk-rock D if grains are < 1 µm. If the rock is composed chiefly of fine-grained material at-or-below this limit, a rock may have a bulk-rock D which is considerably lower than mineralogy or porosity would suggest. If fine grains are concentrated in small patches (e.g., preferentially-altered minerals metamorphosed under low-grade conditions, ooids, etc.), fine-grained material may have a negligible effect on bulk rock D. However, low-D measured in some coarse-grained rocks suggests that fine-grained material concentrated in the rims of large grains may create additional layers of grain-boundary resistance, effectively isolating large, higher-D grains from the rest of the rock matrix, and lowering bulk-rock D.

5.2 A qualitative analysis of mineralogical controls on bulk-rock thermal diffusivity

The primary control on rock D is the dominant mineral(s) within the rock (Whittington *et al.,* 2009; Merriman *et al.,* 2013). Unlike rock C_P, bulk rock D does not *generally* scale with proportions of minerals within the rock. To perform a preliminary analysis of the effects of mineral proportions on bulk-rock D, we examined very low-porosity metamorphic and igneous rocks. Monomineralic rocks broadly reflect the D of the mineral when textural factors such as porosity are controlled for (figure 7). Polymineralic rocks, however, are more complex. Preliminary analysis of rock D measured using the LFA method suggest several potential categories, a description of each which follows.

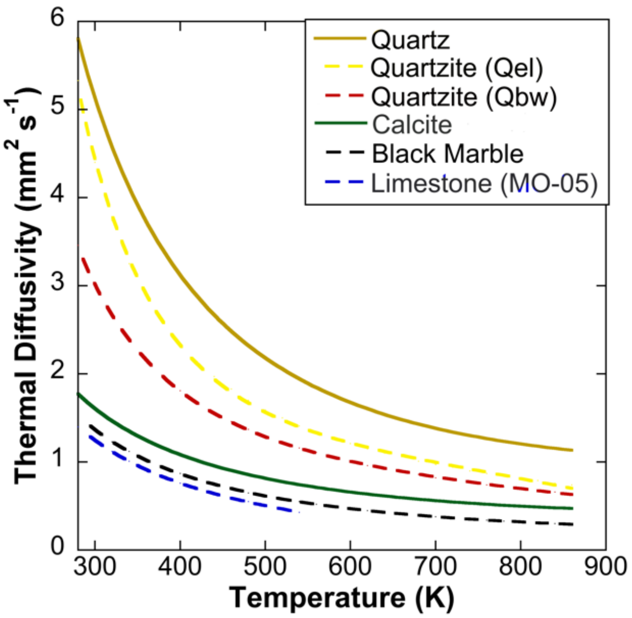

Figure 7) Thermal diffusivity of several monomineralic rocks compared to the directionally-averaged *D* of the dominant mineral within them. Solid lines are minerals, and dashed lines rocks. Quartzites Qel (porosity 5%) and Qbw (porosity 19%) are from Branlund and Hofmeister (2008). Black Marble (Porosity 4%) and Limestone MO-05 (porosity 6%) are from Merriman *et al.* (under review).

5.2.1 Monomineralic and Single-Phase-Dominant Rocks

These are rocks in which all, or most of the mineral volume is composed of a single phase of mineral. Effective *D* of these rocks generally reflects the *D* of the dominant mineral, and scales with pore-space (figure 7). For monomineralic rocks in which the porosity and pore-filling fluid are well-known, bulk-rock *D* can be predicted (at low temperatures) using equation 5. Additionally, because the coefficients of expansion for individual grains are the same, rock-*D* at elevated temperatures is less dampened by differential expansion of grains, meaning the temperature-response of the material is more in-line with nature, where thermal expansion is offset by higher pressures (Hofmesiter, 2006).

5.2.2 Dual-Phase Dominant Rocks

These are rocks in which two mineral phases make up the bulk of the rock volume. Early work suggests that the most abundant mineral phase forms the basis of bulk-rock *D*, but as the ratio of primary vs secondary mineral phases decreases, mixing of mineral *D* occurs. For example, AW20 is a tholeiite basalt from the Wind River Mountains (Wyoming). Merriman *et al.* (2013) measured the *D* of AW20 from 296-1459 K (figure 8). Estimates of mineral proportions by optical microscopy suggest the rock was dominated by low-*D* plagioclase (~50%) and moderately-higher *D* pyroxene (~40%). Across the range of temperatures measured, *D* was ~2-8% higher than directionally-averaged albite, suggesting the plagioclase phase dominates heat transport with a modest increase due to the secondary phase (pyroxene). Similarly, AW16 is a banded iron formation (BIF) from Pilot Knob, Missouri (figure 8). Merriman *et al.* (2013) estimated roughly equal proportions of quartz and hematite in the sample using optical microscopy. Later X-ray diffraction (XRD) results found the sample contained 51% hematite, 33% quartz, 9% muscovite, and 7% barite. The resulting *D* of the sample scales to the weighted average of quartz and hematite with differences between <1% and 8% by temperature.

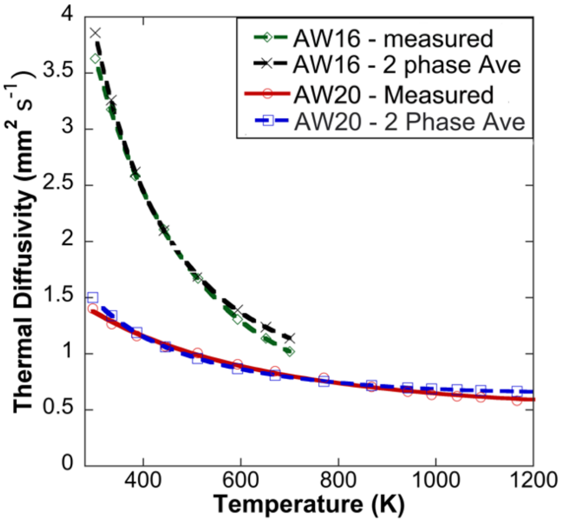

Figure 8) Measured thermal diffusivity and calculated (2 Phase Ave) thermal diffusivity using a weighted average of the two most dominant minerals in a banded iron formation (AW16) and a tholeiitic basalt (AW20). Both samples show a slight departure from mineral averages at elevated temperatures, an effect observed in other rocks which may result from differential expansion of grains opening pore space during heating. Lithostatic (or hydrostatic) pressure may offset this effect in the crust.

5.2.3 Multi- (More Than 2) Phase Dominant Rocks

Rocks in this category have three or more mineral phases in significant proportions. Mixture of *D*'s in these rocks is complex, and will require much more data to analyze bulk-rock *D*. In some cases, weighted averages of the *D* of dominant phases produces near-measured *D* (e.g. KB12, figure 9a), but in others, bulk-rock *D* appears unaffected by the presence of large quantities high-*D* phases (e.g. KB11, figure 9b). Future work will address bulk-rock *D* of multi-phase dominant rocks using larger numbers of samples with tightly-constrained mineralogy (XRD), porosity, and grain-size.

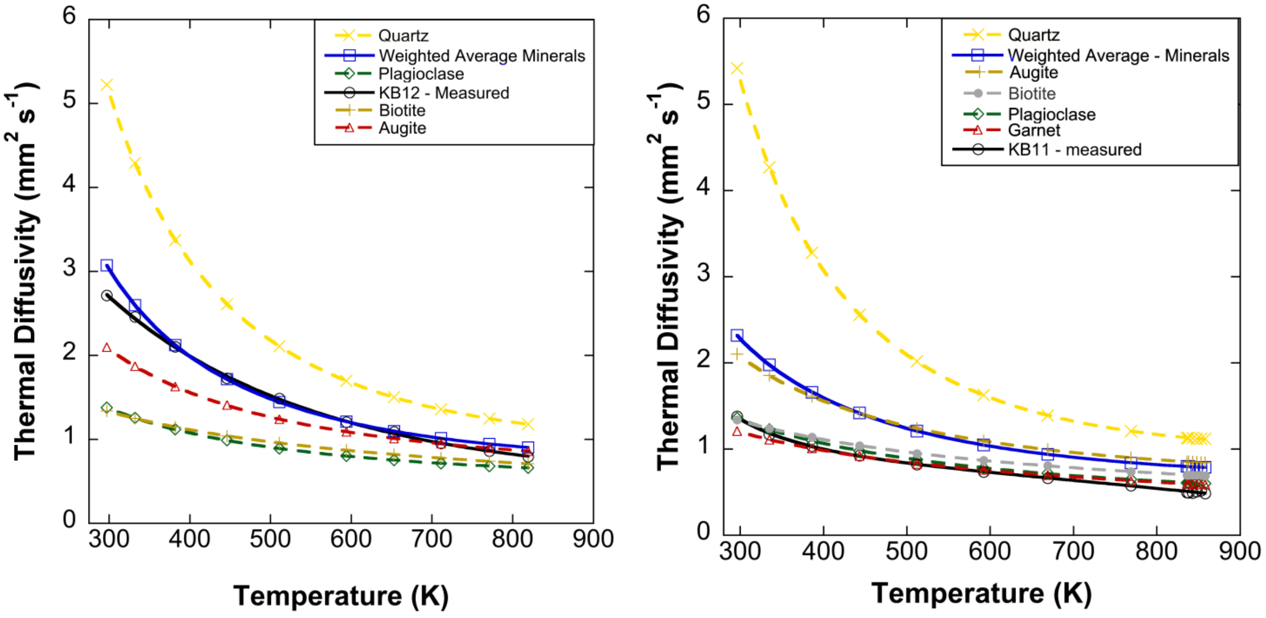

Figure 9) Measured thermal diffusivity (black lines) of rocks KB12 (tonalite) and KB11 (granulite) with directionally-averaged *D* of constituent minerals and weighted averages of the mineral phases (blue lines). KB12 fits well with weighted averages with small departures at low and high temperatures, but KB11 results are inconsistent. KB11 results may be closer if plagioclase within the sample is exceptionally Ca-rich (see section 3).

5.3 Models of temperature-dependence using low-temperature measurements of thermal conductivity

A number of models have been produced to calculate the temperature-response of bulk-rock D from a single room- (or near-room) temperature measurement of rock thermal conductivity (e.g. Lee and Demming, 1998). Figure 10 shows the predicted *dk/dT* for two carbonate rocks using low-T *k* calculated from direct measurement of *D*, C_P, and density (after Merriman *et al.,* under review). In general, these models overestimate *k* at elevated temperatures except in the case of a high-*D* dolomitic marble (figure 10b). This is unsurprising given these models are calibrated with data collected using methods that do not control for ballistic radiative transfer (see section 2). Given the diversity of changes in *D* with temperature for minerals (figure 2), it is unlikely that any single equation will adequately reproduce *D* for all rocks across all relevant temperatures. However, a set of equations calibrated based on rock types with similar mineral sets may reproduce bulk-rock *k* for broader rock-types. Future work will explore possible equations based on the physics of *mineral* heat transport and the effects of textural features in the rock combined with measured C_P and density.

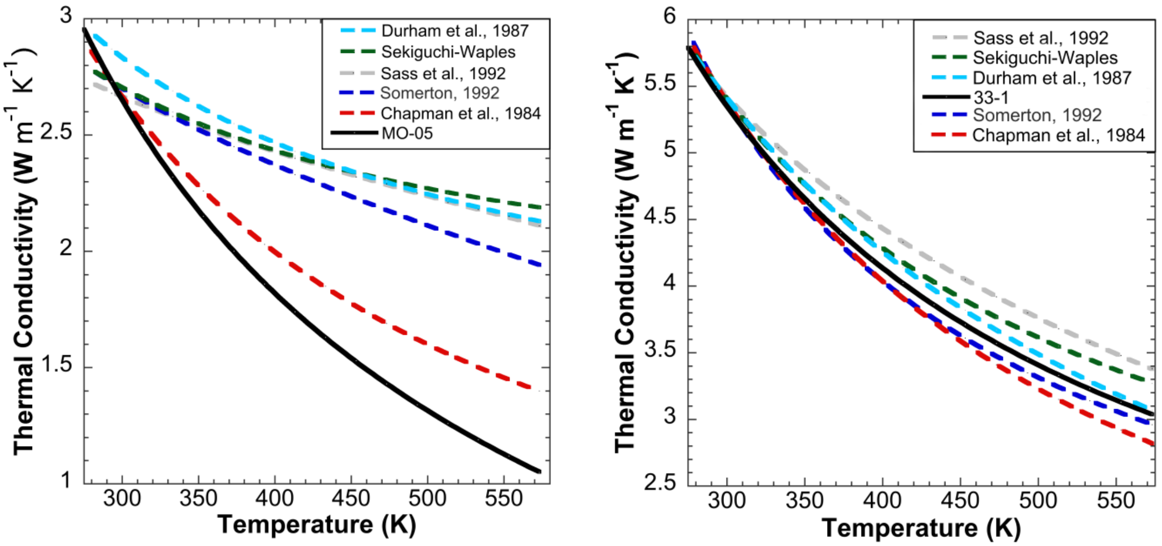

Figure 10) A comparison of the predicted (dashed lines) *dk/dT* of two carbonate rocks MO-05 (Burlington Limestone) and 33-1 (calcite-dolomite-forsterite-chlorite marble) with *k* calculated from direct measurement of *D*, C_P, and density (black lines).

6) CONCLUSIONS

As numerical modeling continues to grow in importance in geothermal exploration and development, better constraints on the physical properties of the lithosphere will provide opportunity for more realistic models. Because many common methods for measuring the ability of lithospheric rocks to conduct heat contain systematic errors, or are restricted to near-surface temperatures despite strong evidence that thermal conductivity and thermal diffusivity change by highly variable amounts at different temperatures. An understanding of the properties that control a rock's ability to conduct heat will aid workers in creating more realistic thermal models in geothermal energy. Broadly, rock *k* is a function of the rock's mineralogy, porosity, and density, but further work is needed to tightly constrain the effects of these properties on bulk-rock *k*, particularly the effects of multiple types of minerals in the same rock. Examining these effects using direct measurement of thermal diffusivity simplifies the problem because the heat capacity, density, and thermal diffusivity can be independently constrained and experimental error is limited.

REFERENCES

Abramson, E.H., Brown, J.M., and Slutsky, L.J.: The Thermal Diffusivity of Water at High Pressures and Temperatures, *Journal of Chemical Physics*, **115** (22), (2001), 10461-10463.

Birch, F., and Clark, H.: The Thermal Conductivity of Rocks and its Dependence Upon Temperature and Composition, *American Journal of Science*, **238** (8), (1940), 529-558.

Branlund, J.M. and Hofmeister, A.M.: Thermal diffusivity of quartz to 1,000°C: effects of impurities and the α-β transition. *Physics and chemistry of minerals*, **34** (8), (2007), 581-595.

Branlund, J.M., and Hofmeister, A.M.: Factors affecting heat transfer in natural SiO_2 solids, *American Mineralogist*, **93**, (2008), 1620-1629.

Branlund, J.M. and Hofmeister, A.M. (2012) Heat transfer in plagioclase feldspars. *American Mineralogist*, **97**, 1145-1154.Carson, J.K., Lovatt, S.J., Tanner, D.J., and Cleland, A.C.: Thermal Conductivity Bounds for Isotropic, Porous Materials, *International Journal of Heat and Mass Transfer*, **48**, (2005), 2150-2158.

Clauser, C., and Huenges, E.: Thermal Conductivity of Rocks and Minerals, *Rock Physics and Phase Relations*: A Handbook of Physical Constants, AGU Reference Shelf 3, The American Geophysical Union, (1995), 105-126.

Gibert, B., Schilling, F.R., Tommasi, A., and Mainprice, D.: Thermal Diffusivity of Olivine Single-Crystals and Polycrystalline Aggregates at Ambient Conditions – a Comparison, *Gophysical Research Letters*, **30** (22), (2003), 2172, doi:10.1029/2003GL018459.

Hantschel, T. and Kauerauf, A.I.: Fundamentals of Basin and Petroleum Systems Modeling. Springer, Dordrecht. (2009)

Hofmeister, A.M.: Thermal diffusivity of garnets at high temperature. *Physics and Chemistry of Minerals*, **33**, (2006), 45-62.

Hofmeister, A.M.: Pressure dependence of thermal transport properties. Proceedings of the National Academy of Sciences, 104, (2007), 9192-9197.

Hofmeister, A.M.: Thermal Diffusivity of Clinopyroxenes at Elevated Temperature, *European Journal of Mineralogy*, **20**, (2008), 537-549.

Hofmeister, A.M.: Scale aspects of heat transport in the diamond anvil cell, in spectroscopic modeling, and in Earth's mantle: Implications for secular cooling. *Physics of the Earth and Planetary Interiors*, **180**, (2010a), 138-147.

Hofmeister, A.M.: Thermal Diffusivity of Oxide Perovskite Compounds at Elevated Temperature, **107** (10), (2010), doi: 10.1063/1.3371815.

Hofmeister, A.M.: Thermal Diffusivity of Orthopyroxenes and Protoenstatite as a Function of Temperature and Chemical Composition, **24** (4), (2012), 669-681.

Hofmeister, A.M.: Thermal Diffusivity and Thermal conductivity of Single-Crystal MgO and Al_2O_3 and Related Compounds as a Function of Temperature, *Physics and Chemistry of Minerals*, **41**, (2014), 361-371.

Hofmeister, A.M., and Pertermann, M.: Thermal Diffusivity of Clinopyroxenes at Elevated Temperature, *European Journal of Mineralogy*, **20** (4), (2008), 537-549.

Hofmeister, A.M., Whittington, A.G. and Pertermann, M.: Transport properties of high albite crystals, near-endmember feldspar and pyroxene glasses, and their melts to high temperature. *Contributions to Mineralogy and Petrology.,* **158**, (2009), 381-400.

Hofmeister, A.M., Dong, J., and Branlund, J.M.: Thermal Diffusivity of Electrical Insulators at High Temperatures: Evidence for Diffusion of Bulk Phonon-Polaritons at Infrared Frequenceies Augmenting Phonon Heat Conduction, *Journal of Applied Physics*, **115**, (2014), doi:10.1063/1.4873295.

Hofmeister, A.M., and Carpenter, P.K.: Heat Transport of Micas, *The Canadian Mineralogist,* **53**, (2015), 557-570.

Hofmeister, A.M., and Ke, R.: Thermal Diffusivity of Feldspathoids and Zeolites as a Function of Temperature. *Physics and Chemistry of Minerals*, **42**, (2015) 693-706.

Hofmeister, A.M. and Branlund, J.M.: Thermal conductivity of the Earth. *Treatise on Geophysics*, **2**, (2015), 543-577.

Lawson, A.W., Lowell, R., and Jain, A.L.: Thermal Conductivity of Water at High Pressures, **30**, (1959), 643

Lee, Y. and Deming, D.: Evaluation of thermal conductivity temperature corrections applied in terrestrial heat flow studies. *Journal of Geophysical Research*, **103** (B2), (1998), 2447-2454.

Mehling, H., Hautzinger, G., Nilsson, O., Fricke, J., Hofmann, R. and Hahn, O.: Thermal diffusivity of semitransparent materials determined by the laser-flash method applying a new mathematical model. *International Journal of Thermo- physics*, **19**, (1998), 941–949.

Merriman, J.D., Whittington, A.G., Hofmeister, A.M., Nabelek, P.I. and Benn, K.: Thermal transport properties of major Archean rock types to high temperature and implications for cratonic geotherms. *Precambrian Research*, **233**, (2013), 358-372.

Merriman, J.D., Hofmeister, A.M., Roy, D.J., and Whittington, A.G.: Temperature-Dependent Thermal Transport Properties of Carbonate Minerals and Rocks, submitted to *Basin Research*, December, 2016, (Under Review).

Miao, S.Q., Li, H.P. and Chen, G., Temperature dependence of thermal diffusivity, specific heat capacity, and thermal conductivity for several types of rocks. *Journal of Thermal Analysis and Calorimetry*, **115**, (2014), 1057-1063.

Nabelek, P.I., Whittington, A.G. and Hofmeister, A.M.: Strain heating as a mechanism for partial melting and ultrahigh temperature metamorphism in convergent orogens: Implications of temperature-dependent thermal diffusivity and rheology. *Journal of Geophysical Research*, **115**, (2010), B12417.

Nabelek, P.I., Hofmeister, A.M., and Whittington, A.G.: The Influence of Temperature-Dependent Thermal Diffusivity on the Conductive Cooling Rates of Plutons and Temperature-Time Paths in Contact Aureoles, **317-318**, (2012), 157-164.

Parker, J.W., Jenkins, J.R., Butler, P.C. and Abbott, G.I., Flash method of determining thermal diffusivity, heat capacity, and thermal conductivity. *Journal of Applied Physics*, **32**, (1961), 1679-1684

Pertermann, M., Whittington, A.G., Hofmeister, A.M., Spera, F.J. and Zayak, J., Transport properties of low-sanidine single-crystals, glasses and melts at high temperature. *Contributions to Mineralogy and Petrology*, **155** (6), (2008), 689-702.

Popov, Y.A., Pribnow, D.F.C., Sass, J.H., Williams, C.F. and Burkhardt, H., Characterization of rock thermal conductivity by high-resolution optical scanning. *Geothermics*, **28**, (1999), 253-276.

Robertson, E.G., Thermal properties of rocks, United States Department of the Interior, Geological Survey, Open-File Report 88-441, Reston, Virginia, (1988), p. 106.

Robie, R.A. and Hemmingway, B.S., Heat capacities and entropies of Mg_2SiO_4, and Co_2SiO_4 between 5 and 380K. *American Mineralogist*, **67**, (1994), 470-482.

Ross, R.G., Andersson, P., Sundqvist, B., and Backstrom, G.: Thermal Conductivity of Solids and Liquids Under Pressure, *Reports on Progress in Physics*, **47**, (1984), 1347-1402.

Schütz, F., Norden, B. and Förster, A.: Thermal properties of sediments in southern Israel: a comprehensive data set for heat flow and geothermal energy studies. *Basin Research,* **24**, (2012), 357-376.

Smith, D.S., Fayette, S., Grandjean, S. and Martin, C.: Thermal resistance of grain boundaries in alumina ceramics and refractories. *Journal of American Ceramics Society,* **86**, (2003), 105-111.

Wang, J., Carson, J.K., North, M.F., and Cleland, D.J.: A New Structural Model of Effective Thermal Conductivity for Heterogeneous Materials With Co-continuous Phases, *International Journal of Heat and Mass Transfer*, **51**, (2008), 2389-2397.

Whittington, A.G., Hofmeister, A.M. and Nabelek, P.I.: Temperature-dependent thermal diffusivity of Earth's crust: Implications for crustal anataxis. *Nature*, **458**, (2009), 319-321.

Yu, X., and Hofmeister, A.M.: Thermal Diffusivity of Alkali and Silver Halide Crystals as a Function of Temperature, **109** (3), (2011), doi: 10.1063/1.3544444